Light: Science & Applications (2012) 1, e22; doi:10.1038/lsa.2012.22

www.nature.com/lsa

ORIGINAL ARTICLE

High-brightness polarized light-emitting diodes

Elison Matioli[1], Stuart Brinkley[2], Kathryn M Kelchner[2], Yan-Ling Hu[3], Shuji Nakamura[2,3], Steven DenBaars[2,3], James Speck[3] and Claude Weisbuch[3,4]

Light-emitting diodes are becoming the alternative for future general lighting applications, with huge energy savings compared to conventional light sources owing to their high efficiency and reliability. Polarized light sources would largely enhance the efficiency in a number of applications, such as in liquid-crystal displays, and also greatly improve contrast in general illumination due to the reduction in indirect glare. Here, we demonstrate light-emitting diodes presenting high-brightness polarized light emission by combining the polarization-preserving and directional extraction properties of embedded photonic-crystals applied to non-polar gallium nitride. A directional enhancement of up to 1.8-fold was observed in the total polarized light emission together with a high polarization degree of 88.7% at 465 nm. We discuss the mechanisms of polarized light emission in non-polar gallium nitride and the photonic-crystal design rules to further increase the light-emitting diode brightness. This work could open the way to polarized white-light emitters through their association with polarization-preserving down-converting phosphors.
Light: Science & Applications (2012) **1,** e22; doi:10.1038/lsa.2012.22; published online 3 August 2012

Keywords: GaN; LEDs; *m*-plane; polarized light

INTRODUCTION

Due to a continuously improved performance, light-emitting diodes (LEDs) are not only the major contender for future general lighting sources,[1] but also play an important role in a growing number of other applications—from backlight for high-efficiency televisions and mobile phone displays, to car lights and headlights—replacing the classical white sources owing to their high efficiency, brightness, reliability and low operation cost. Polarized light sources would largely improve the efficiency of most of these applications: from general illumination, with an improved contrast due to reduced glare,[2] which also minimizes eye discomfort and ultimately eye strain,[3] to high-efficiency displays which operate through the spatial modulation of polarized light[4] (for completeness, we also note that polarized light and other forms of artificial light could be harmful for the life of animals and other species relying on natural light cycles to live[5]). However, common light sources are usually unpolarized, since the electric field of the light emitted has no preferred orientation. This is also the case for most of the nitride-based LEDs commercialized nowadays. A strongly linearly polarized source, however, is obtained in *m*-plane GaN LEDs where the asymmetric in-plane biaxial stress on the quantum wells (QWs) orients the light emitting dipoles preferentially along the in-plane *a* direction. Non-polar *m*-plane GaN LEDs were first developed and more intensively investigated due to the possible reduction of polarization-induced electric fields in the QWs, which for *c*-plane GaN LEDs degrade their radiative recombination rate as a result of quantum confined stark effects.[6,7] Today, the availability of high-quality free-standing substrates along non-polar and semipolar crystal planes of GaN allowed the demonstration of high-effciency optoelectronic devices.[8,9]

High polarization ratios (defined in equation (1)) have been reported in *m*-plane GaN LEDs,[10–13] however, such LEDs present poor light-extraction efficiency due to total internal reflection at the flat GaN/air interface. The common light-extraction improving schemes applied to LEDs rely on randomizing the light reflected off the interfaces (roughened interfaces[14] or patterned substrates[15]) which increases the light output of *m*-plane LEDs but also randomizes the original intrinsic polarization of the emitted light. The diffraction of light by optical gratings (or photonic crystals (PhCs)) offers one possible polarization-preserving light-extraction mechanism, in addition to the high light-extraction efficiency demonstrated in GaN LEDs.[16,17]

In this work, we embed periodically distributed air rods (embedded PhCs) within the LED structure to form a highly diffractive optical medium that offers high light-extraction efficiency. The coherent nature of the diffraction by PhCs not only retains the original polarization of light but also offers directional light extraction, resulting in high-brightness polarized LEDs. We develop a theoretical model of light emission in *m*-plane GaN and of its interaction with PhCs, and discuss the important parameters to design and enhance the directional polarized light emission. We demonstrate highly polarized emission with a degree of polarization of 88.7% at 465 nm and enhancement up to 1.8-fold in directional polarized emission. We show that more than increasing the polarized light emission, PhCs

[1]Department of Electrical Engineering and Computer Science, Massachusetts Institute of Technology, Cambridge, MA, USA; [2]Department of Electrical and Computer Engineering, University of California, Santa Barbara, CA, USA; [3]Materials Department, University of California, Santa Barbara, CA, USA and [4]Laboratoire de Physique de la Matière Condensée, CNRS, Ecole Polytechnique, Palaiseau, France
Correspondence: Dr E Matioli, Department of Electrical Engineering and Computer Science, Massachusetts Institute of Technology, 77 Massachusetts Avenue, Rm 39-663, Cambridge, MA 02139, USA
E-mail: elison.matioli@polytechnique.org
Received 13 January 2012; revised 7 May 2012; accepted 10 May 2012

offer a tool to control and design the angular emission pattern of LEDs. The association of such high-brightness polarized blue LEDs with polarization-preserving down-converting phosphors,[18] such as oriented dye systems[19] or quantum dashes,[8] could open the way to polarized white-light emitters.

MATERIALS AND METHODS

Embedded PhC fabrication

The reported devices were grown by metal-organic chemical vapor deposition (MOCVD) on commercially available free-standing *m*-plane GaN substrates with −1° miscut. The one-dimensional (1D) PhCs with period a'=270 nm and depth of ~160 nm were patterned on the surface of the *m*-plane substrates by interference lithography using THMR-M100 photoresist, XHRiC-16 anti-reflective coating and a 220-nm-thick SiO_2 hard mask deposited over GaN. The stripes were transferred to GaN by inductive coupled plasma. After the removal of the lithography resist and the SiO_2 hard mask, the GaN patterned substrate was ready for the MOCVD growth. The coalescence of a thin layer over the air-groove stripes aligned parallel to the *a* direction was achieved, using a similar method of Ref. 20 adapted to m-plane GaN. Its detailed description will be reported later.

LED fabrication

The LED structure consisted of a ~1-μm-thick Si-doped n-GaN layer, followed by 3× InGaN/GaN (4/10 nm) QW/barriers, a 15-nm-thick Mg-doped $Al_{0.18}Ga_{0.82}N$ electron-blocking layer and a 200-nm-thick Mg-doped p-GaN. Layer thicknesses and compositions were estimated from X-ray diffraction on calibration samples, grown separately. An *m*-plane substrate without PhCs was coloaded in the same LED growth run for comparison. The LEDs were processed on both samples using a 250-nm-thick indium tin oxide as transparent contact layer to the p-GaN. Individual mesas were etched through the active layers to reach the n-type GaN using inductive coupled plasma etch. The n-type contact layer consisted of an annealed metal stack of Ti, Al, Ni and Au (10/100/10/100 nm). Contact pads were formed using Ti/Au (15/350 nm), deposited by electron beam evaporation.

Optical characterization

The diffraction of polarized guided light by the PhCs was assessed by polarized angle-resolved spectral measurements, where the spectrum of the LED under electric bias was measured by a rotating optical fiber at angles θ from −90° to 90° (0° being the vertical direction normal to the LED). A polarizer was placed in front of the optical fiber to select between the $\vec{E}||\vec{a}$ and $\vec{E}||\vec{c}$ polarizations. The samples were measured on wafer with adjacent LEDs covered using an aperture that exposed only the device of interest. This procedure eliminated most of the scattered light from the sidewalls and from the other devices; however, in the angle-resolved measurements, it is expected that a small portion of the light could still be scattered by the sidewalls of the LEDs mesas (~600 nm of height), which reduces the measured polarization ratio. The backside of the wafers was polished to minimize scattering and depolarization of the emitted light. The LEDs were driven at 2 mA. Recent reports in the literature showed that the polarization ratio in *m*-plane GaN LEDs is nearly independent of current density,[13] and a large polarization ratio can be maintained over a wide range of current densities from 0.5 to 1000 $A{\cdot}cm^{-2}$, which is important for lighting applications where LEDs are usually operated at high current densities.

To precisely determine the polarization ratio using equation (1), the sidewalls, backside and part of the top surface of the devices were covered with light absorbing material based on carbon nanoparticles (Superior Graphite Co., Chicago, IL, USA) to eliminate the collection of extra scattered light.[11,13,21]

POLARIZED EMISSION IN *M*-PLANE GAN LEDS: ELECTRIC DIPOLE DESCRIPTION

Spontaneous radiative recombination from electrons in the conduction band (CB), with atomic *s* orbital character, and holes in the valence bands (VB), with atomic p_x, p_y and p_z orbital characters (Figure 1a), is given by Fermi's golden rule and is proportional to the quantum mechanical dipole moments between these states. The correspondence principle states that these quantum mechanical dipole moments are well described by electric oscillating dipole moments from classic electromagnetism,[22] oriented parallel to the direction of the corresponding *p* orbital.

For InGaN QWs grown on *m*-plane GaN, the anisotropic compressive biaxial stress in the QWs breaks the symmetry of the original $|X\pm iY\rangle$-like heavy and light-hole valence bands of unstrained wurtzite GaN, into $|X\rangle$- and $|Y\rangle$-like bands. The compressive stress raises the $|X\rangle$ state and lowers the $|Y\rangle$ state below the spin-orbit crystal-field splitting $|Z\rangle$ band (Figure 1a), resulting in a smaller energy of the interband transitions between CB and $|X\rangle$ compared to that between CB and $|Y\rangle$.[23]

In such QWs, the more intense emission comes from the lower energy CB–$|X\rangle$ recombinations corresponding to *x*-oriented dipoles, P_x, radiating an electric field $\vec{E}$ mostly parallel to the *a* direction, while the less intense CB–$|Z\rangle$ recombination yields a P_z dipole, emitting mostly in the *x*–*y* plane with an electric field polarized along *c*.[11,24] The even less intense CB–$|Y\rangle$ recombination corresponds to P_y dipoles

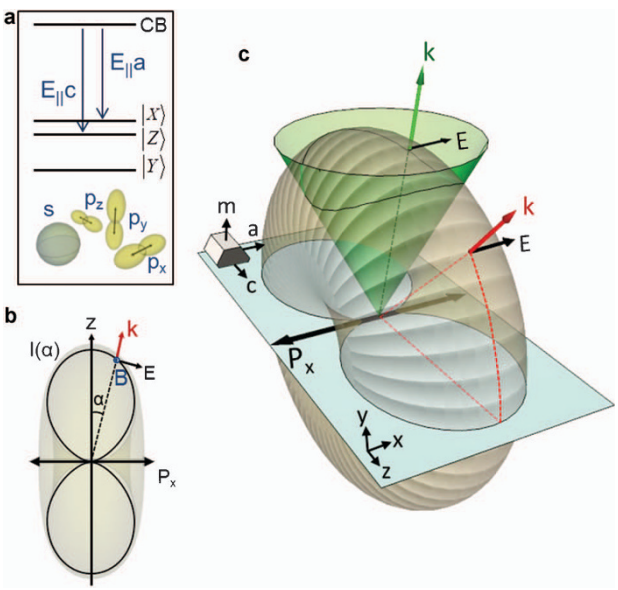

Figure 1 Light emission from *m*-plane InGaN QWs. (**a**) Schematic of the orientation of the atomic orbitals and the conduction and valence bands in compressively strained *m*-plane GaN. (**b**) Top view of the radiation pattern of a single dipole along *a* indicating the wavevector $\vec{k}$, electric $\vec{E}$ and magnetic $\vec{B}$ fields, both proportional to cosα and the radiated intensity $I(\alpha)\sim\cos^2\alpha$. (**c**) Three-dimensional representation of the single dipole-like radiation pattern (torus) from an *m*-plane QW. The P_x dipole radiates polarized light to air through the air cone. The emission outside the air cone excites polarized guided light in the semiconductor slab. The plane represents the QWs and the complete LED structure is not shown for simplicity. LED, light-emitting diode; QW, quantum well.

radiating electric field mostly along the *m* direction (negligible emission compared to the other two dipoles).

The difference between the intensities emitted vertically from the dipoles is quantified by the polarization ratio, defined as

$$\rho = \left(I_{||a} - I_{||c}\right) / \left(I_{||a} + I_{||c}\right) \quad (1)$$

where $I_{||a}$ and $I_{||c}$ are the intensities of light polarized along the *a* and *c* directions emitted in the vertical direction.

In *m*-plane InGaN QWs where high polarization ratios have been reported—~92% at wavelengths of 485 nm[12] and even higher at longer wavelengths[13]—the intensity emitted from the *a*-oriented dipole can be 20 times higher than that emitted from the *c*-oriented dipole. Therefore, the light emitted in *m*-plane GaN can be treated to very good approximation by a single emitting dipole along the *a* direction of the plane. This is a unique property in solid-state light-emitters: *m*-plane GaN LEDs radiate as a macroscopic single dipole. Oscillating electric dipoles radiate in the far-field radially in all directions. The electric field $\vec{E}$ lies in the same plane of the dipole and the magnetic field $\vec{B}$ is perpendicular to this plane (Figure 1b). The amplitude of these fields is proportional to cosα (intensity proportional to $\cos^2\alpha$), being most intense at the directions perpendicular to the dipole and vanishing along the dipole axis. The direction of the Poynting vector $\vec{S}$ is radial, perpendicular to $\vec{E}$ and $\vec{B}$ (Figure 1b). In three dimensions, the radiation pattern of the main dipole P_x follows a torus (Figure 1c). Light emitted with angles within the air cone (green cone) is radiated to air (green wave vector), and the emission outside the air cone excites guided light in the semiconductor slab (red wave vector). The guided modes are polarized by the dominant emission with $\vec{E}||\vec{a}$ and propagate mainly perpendicularly to the orientation of the dipole.

To be relevant for applications, one needs to enhance the emission of polarized light from *m*-plane GaN LED, since only the small fraction of light emitted within the air cone is radiated to air. The single dipole-like emission of *m*-plane QWs motivates the use of 1D PhCs aligned along the *a* direction (perpendicular to the preferential plane of propagation of the guided modes), which act as a diffraction grating for the polarized guided modes, out-coupling them to air (treated in more details in the last section of this paper). To effectively extract the guided light in the rather thick free-standing *m*-plane GaN substrates, the PhCs were placed within the LED structure, which increases their interaction with the guided modes (schematics in Figure 2a).[25] An improved diffraction efficiency is obtained by embedding air gaps within the GaN, which results in a large contrast in refractive index. The extraction of polarized light by embedded PhCs in *m*-plane GaN LEDs was further motivated by the high extraction efficiency previously observed in *c*-plane GaN LEDs.[17]

DIRECTIONAL ENHANCEMENT OF POLARIZED LIGHT EMISSION

The fabrication of embedded PhCs relied in a simple process, consisting of patterning a free-standing *m*-plane GaN substrate with grooves by dry etch followed by a quick growth by MOCVD to coalesce a thin layer of *m*-plane GaN over the air-gap PhCs (see the section on 'Materials and methods'). The coalescence was mainly determined by the growth rates and stability of different crystallographic facets of GaN upon specific growth conditions,[20] it did not rely on the deposition of growth-blocking material inside the air gaps. Figure 2a and 2b shows the schematic of the LED structure and the transmission electron microscopy image revealing the coalescence of a 290-nm-thick defect-free layer over the air grooves. This is an important result, especially for optoelectronic devices, where some

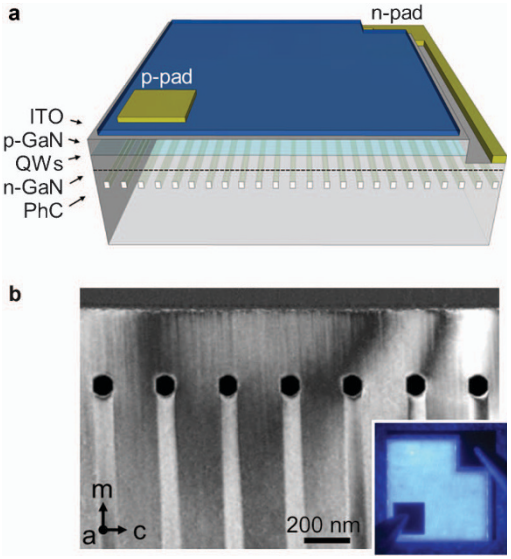

Figure 2 Embedded PhC LEDs in *m*-plane GaN. (**a**) Schematic of the LED structure (not in scale). (**b**) TEM image of the cross-section of the embedded PhC structure showing a defect-free coalesced layer over the air-grooves (corresponding to the region below the dashed line in **a**). The features observed below the air grooves are artifacts from the focused ion beam used to prepare the sample for TEM measurement. The inset shows a top-view image of the embedded PhC LED under bias. ITO, indium tin oxide; LED, light-emitting diode; PhC, photonic crystal; TEM, transmission electron microscope.

defects can act as non-radiative recombination centers which reduce the overall quantum efficiency of the device. LED structures were grown over both the *m*-plane substrates with embedded PhCs and without PhCs, coloaded in the same LED growth run for comparison. A picture of the embedded PhC LED under bias, processed as described in the section on 'Materials and methods', is shown in the inset of Figure 2b.

The extraction of polarized guided light by the embedded PhCs was assessed by angle-resolved spectral measurements (see the section on 'Materials and methods'). Figure 3a shows such measurement for both devices combined in a single image, where $\theta = 0^\circ$ is the vertical direction normal to the LED. The sample without PhCs (Figure 3a) shows the regular angular emission pattern of a flat surface LED, corresponding to the emission of dipoles in a quasi semi-infinite medium through a flat top surface of the LED, which results in the absence of Fabry–Perot fringes in the experimental data. For the embedded PhC LED, the angle-resolved measurement reveals the extraction of different guided modes with $\vec{E}||\vec{a}$ polarization, represented by the sharp lines in the left-hand side of Figure 3a. The measured radiation is composed of direct polarized emission within the air cone from the non-polar QWs, as for the sample without PhCs, plus the extra polarized light from the extracted guided modes.

The intensity versus angle at the peak wavelength for both $\vec{E}||\vec{a}$ and $\vec{E}||\vec{c}$ polarizations is shown in Figure 3b, where the enhancement in $\vec{E}||\vec{a}$-polarized emission by the embedded PhC LED can be more clearly observed. The emission of the $\vec{E}||\vec{c}$ polarization is nearly unchanged by the embedded PhCs due to the preferential extraction of polarized guided modes propagating perpendicularly to the 1D embedded PhCs ($\vec{E}||\vec{a}$-polarized guided modes). The small changes on the $\vec{E}||\vec{c}$ polarization observed in Figure 3c are attributed mainly to scattering of the stronger $\vec{E}||\vec{a}$ polarization at sidewalls and neighboring devices which depolarizes the scattered light and contributes

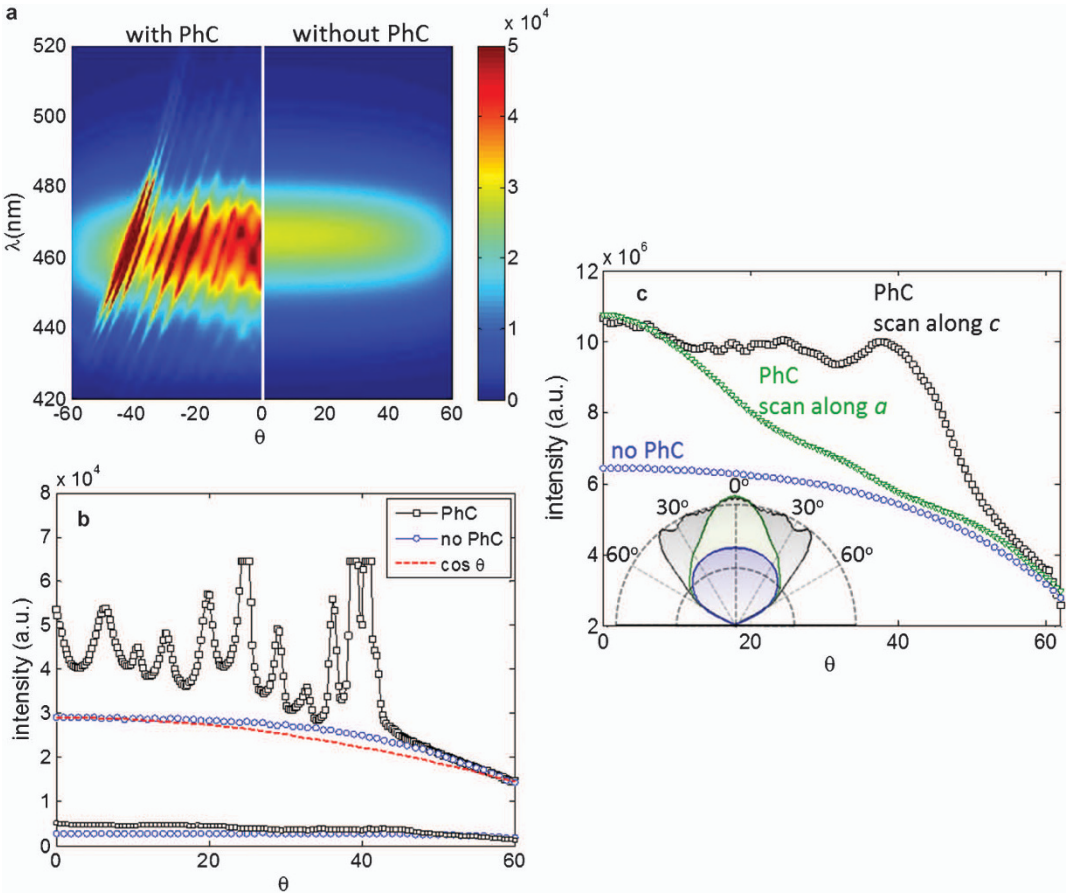

Figure 3 Optical characterization of polarized emission. (**a**) Comparison of angle-resolved measurements along the *m*–*c* plane for the $\vec{E}||\vec{a}$-polarized spectra, for LEDs with (left hand side) and without embedded PhCs (right hand side). The radiation from embedded PhC LED is composed of direct polarized emission (similar to the LED without PhCs), plus the extra polarized light from the extracted guided modes. A slight shift in the emission wavelength was observed between the embedded PhC (465 nm) and the LED without PhCs (470 nm). (**b**) Intensity versus angle at the peak wavelength for both $\vec{E}||\vec{a}$ and $\vec{E}||\vec{c}$ polarizations, scanned along the *m*-*c* plane. A directional enhancement in $\vec{E}||\vec{a}$-polarized emission is observed due to the extraction of polarized modes by the embedded PhCs whereas only slight changes are observed for the $\vec{E}||\vec{c}$ polarization. The direct light emission can be written as $I_{a,direct}(\theta) \propto \cos\theta$ (see Supplementary Information). (**c**) Integrated angle-resolved measurement of the $\vec{E}||\vec{a}$ polarization, in wavelength, for the LEDs without and with embedded PhCs scanned along the *m*–*c* and *m*–*a* planes of GaN. A plot in polar coordinates is shown in the inset revealing the directional enhancement for the $\vec{E}||\vec{a}$ polarization along both *m*–*c* and *m*–*a* planes. LED, light-emitting diode; PhC, photonic crystal.

to increase the weak emission from $\vec{E}||\vec{c}$ polarization. This effect was later minimized by covering the sidewalls, backside and part of the top surface of the devices with light absorbing material[11,13,21] (see the section on 'Materials and methods'). The observation of a clear mode dispersion demonstrates the preservation of polarization of the guided modes extracted by the embedded PhCs. The embedded PhC LED presented a high polarization ratio of 88.7% (see the section on 'Materials and methods'), which was similar to the sample without PhC. This quantity, however, does not fairly reflect the enhancement in polarized light emission because, by definition, it accounts only for intensities at vertical emission. Moreover, the polarization ratio as defined in equation (1) is sensitive to the presence (or absence) of peaks from the extracted modes by the PhCs at 0°. These results show that the embedded PhCs enhance the total polarized light emission maintaining the high intrinsic polarization ratio of *m*-plane GaN LEDs. The directional extraction of polarized light by the embedded PhCs is seen in Figure 3b, where the enhancement in polarized light emission is observed for angles up to 43°, and beyond that the emitted intensity is similar for both samples. The directional light emission from the embedded PhC LED was quantified by integrating the angle-resolved measurement in wavelength, as shown in Figure 3c, where the peaks from the extraction of guided modes observed in Figure 3b were averaged, forming a plateau up to 43°. An enhancement up to 1.8-fold was observed in the integrated emission of the $\vec{E}||\vec{a}$ polarization, measured along the *m*–*c* plane of the embedded PhC LED. A directional extraction of $\vec{E}||\vec{a}$ polarization was also observed along the *m*–*a* plane (green triangles in Figure 3c). The enhancement in brightness of the $\vec{E}||\vec{a}$-polarized emission is shown in polar coordinates in the inset of Figure 3c. The detailed explanation of these results and the PhC design rules for a directional polarized light emitter are given in the next section.

PHOTONIC-CRYSTAL DESIGN RULES

The small fraction of the polarized emission from the P_x dipole going inside the air cone is radiated to air, the remainder excites preferentially $\vec{E}||\vec{a}$-polarized guided modes propagating mostly in the *y*–*z* (*m*–*c*) plane (α=0). The excitation of guided modes propagating off this plane with angle α (generally referred here as off-axis direction) is reduced according to the toroidal emission pattern from the dipole (intensity proportional to $\cos^2\alpha$). For a given wavelength λ in air, the

wave vector emitted by the dipole inside the semiconductor slab (refractive index n_{GaN}) is $n_{GaN}k_0$, and its projection in the x–z (a–c) plane is $k_{||}=n_{GaN}k_0\sin\theta_i$, where θ_i is the internal angle between the wave vector and the vertical direction. When the magnitude of the in-plane wave vector $k_{||}$ is smaller than the in-plane projection of the air cone, defined as a circle of radius $k_0=2\pi/\lambda$, the wave is radiated to air. On the other hand, if $k_{||}>k_0$, the wave stays inside the semiconductor slab as polarized guided light.

In the present case, the embedded air gaps form a layer of lower effective index of refraction within the LED structure which creates a thin waveguide above the PhCs.[26] A discrete set of nine guided modes is supported (Figure 4a) with effective indices $n_{effective}$ (where $n_{effective}=k_{||}/k_0$) between n_{GaN} ~2.41 and n_{PhC} ~2.03 (see Supplementary Information). The calculated dispersion relation of these modes, which corresponds to the in-plane wave vector $k_{||}$ guided in this waveguide structure for a given wavelength λ, is shown in Figure 4b.

PhCs (or optical gratings) diffract-guided modes by modifying their in-plane wave vector $\vec{k}_{||,m}=\vec{k}+m\vec{G}$, where $\vec{G}$ is the PhC reciprocal vector ($G=2\pi/a'$ for 1D PhCs and a' is the PhC period) and m is an integer. A guided mode is diffracted to air, along with its original polarization, when one of its infinite set of harmonics $\vec{k}_{||,m}$ is within the air cone,[27] or $|\vec{k}_{||,m}|<k_0$ (Figure 4a). The original polarization of the direct light and guided modes is not disturbed, neither by the LED structure, nor by the PhCs, since their different interfaces are parallel to each other, as well as to the direction of the main electric field $\vec{E}||\vec{a}$, denoted by E_a (see Supplementary Information).[28,29] Figure 4a shows the electric field profile of three of the guided modes supported in the thin waveguide diffracted by the PhCs. The diffracted in-plane wave vectors are conserved in different media, and different guided modes are diffracted by the PhCs at different well defined angles. For a given PhC design (given G), the low order mode (blue in Figure 4a) is diffracted with a $k_{||,-1}$ close to the edge of the air cone (k_0), therefore propagating at a glancing angle in air. The other extreme is depicted by the high order mode (green), where the diffracted in-plane wave vector $k_{||,-1}$ is zero, resulting in a diffracted wave vector along the vertical direction. The effect of the PhC diffraction can also be seen in the calculated dispersion relation of the guided modes. Guided modes are extracted to air when diffracted by $-\vec{G}$ inside the air cone, shown in dashed-lines in Figure 4b, which corresponds to the modes experimentally observed in Figure 3a, where $k_{||,-1}$ is converted into θ by $\theta=\arcsin(k_{||,-1}/k_0)$.

For a more complete analysis, one should also look at the projection of the air cone and wave vectors in the plane of the PhCs (x–z plane) shown in Figure 4c. Guided modes are represented by a circle of radius $k_{||}$ (black semicircles), and their diffracted wave vector by the dashed-red semicircles in Figure 4c. 1D PhCs can be directly described in this in-plane wave vector representation by dots spaced by $\vec{G}$. Along the c direction, the incident guided mode, with in-plane wave vector $k_{||}$ and polarization E_a, is diffracted by the PhC reciprocal vector $-\vec{G}$, resulting in a diffracted in-plane wave vector $k_{c,-1}$ (solid-red vector). The magnitude of $k_{c,-1}$ varies with the ratio a'/λ, which determines the angle of diffraction of a mode and ultimately gives the PhC control over the direction of the diffracted light. For the present values of a' and λ, the first low order guided mode, with $n_{effective}\sim n_{GaN}$, determines the maximum angle at which the directional enhancement of light extraction occurs. Along the m–c plane, this angle is written as $\theta_e=\arcsin(k_{c,-1}/k_0)$ (Figure 5a) which can be approximated by

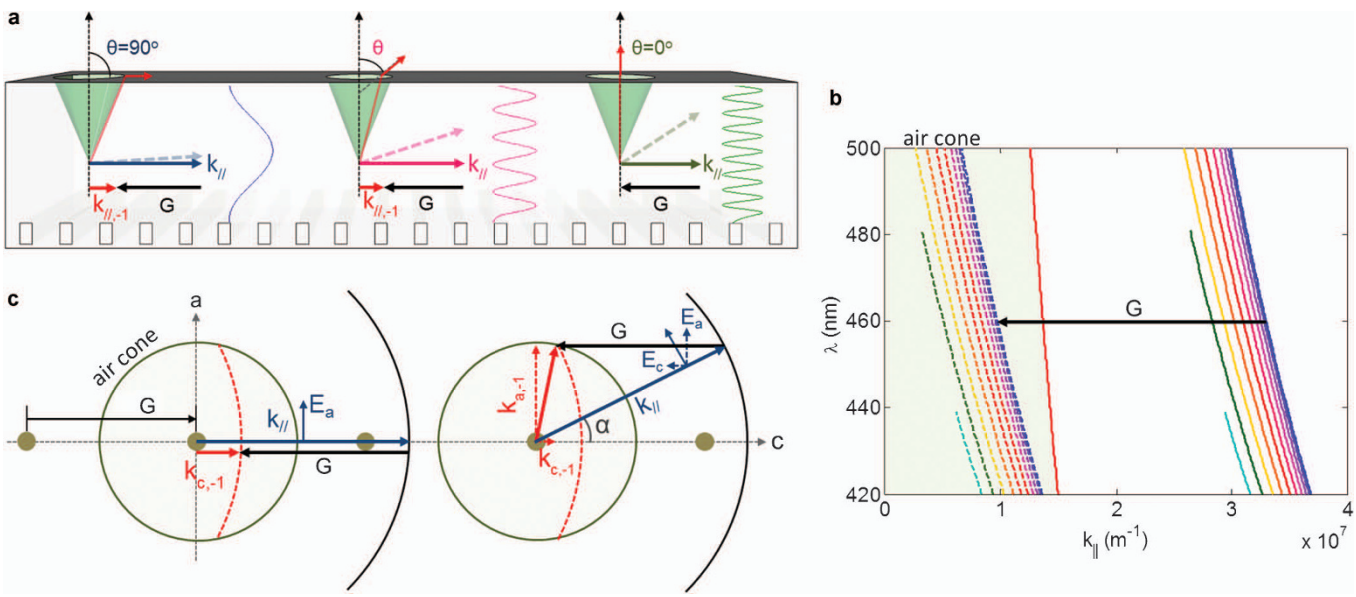

Figure 4 Guided mode diffraction by PhCs. (**a**) Schematics of the single cavity formed in the layer above the embedded PhCs (not in scale) along with the electric field profile of three confined guided modes: a low (blue), a mid (pink) and a high (green) order modes, their in-plane ($k_{||}$) and diffracted ($k_{||,-1}$) wave vectors, and the PhC reciprocal vector G. The low order mode, which propagates originally in a glancing angle, is diffracted with a $k_{||,-1}$ close to the edge of the air cone (k_0), therefore with a glancing angle in air (θ=90°), while the mid-order mode is diffracted at a smaller angle. The other extreme case is depicted by the high order mode, where $k_{||}$ is equal to G ($k_{||,-1}$=0), resulting in a diffracted wave vector along the vertical direction (θ=0°). (**b**) Calculated dispersion relation of all guided modes confined in the top layer above the PhCs. These modes are diffracted by the PhC reciprocal vector $\vec{G}$ inside the air cone, which correspond to the modes observed in Figure 3, where $k_{||,-1}$ is converted into θ by $\arcsin(k_{||,-1}/k_0)$. (**c**) In-plane PhC reciprocal space, represented by the dots, showing the diffraction of polarized guided light within the air cone (red-dotted semicircles). Along the c direction (left), the incident guided mode with in-plane wave vector $k_{||}$ (solid-blue) and polarization E_a is diffracted by the PhC reciprocal vector $-\vec{G}$, resulting in a diffracted in-plane wave vector $k_{c,-1}$ (solid-red). Modes propagating off-axis (right) are also diffracted by 1D PhCs, in both the m–c and m–a planes (dotted-red wave vectors). These modes have polarization components E_a and E_c in both directions, which are diffracted to air. 1D, one-dimensional; PhC, photonic crystal.

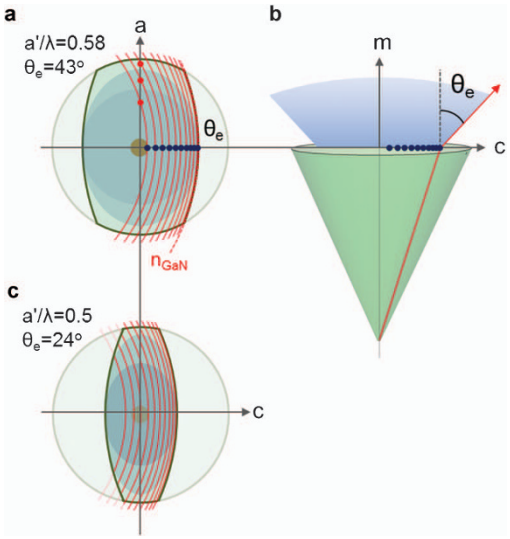

Figure 5 Directional diffraction of guided modes by PhCs. (**a**) Top view of the air cone showing the diffraction of all guided modes supported in the embedded PhC LED within the air cone for a'/λ ratios of 0.58. The blue dots correspond to modes diffracted in the *m*–*c* plane, and the red dots to modes diffracted in the *m*–*a* plane. The lowest order mode defines the angle at the limit of diffraction $\theta=\theta_e$, which in this case is 43°. (**b**) Cross-sectional view of the air cone showing more clearly the light extraction angle θ_e and the directional emission of polarized light. (**c**) In-plane PhC reciprocal space for a'/λ ratios of 0.5, which results in a more directional extraction of polarized guided modes, with $\theta_e=24°$. LED, light-emitting diode; PhC, photonic crystal.

$$\theta_e \approx \arcsin(n_{GaN} - \lambda/a') \quad (2)$$

For $a'/\lambda=0.58$, θ_e is equal to 43°, in agreement with the measurements in Figure 3b.

To increase the directional emission through a vertical extraction of the polarized guided light, the PhC period needs to be designed such that the diffracted $k_{c,-1}$ is zero. Since the structure supports several guided modes and $k_{c,-1}$ is different for each mode, this condition cannot be met by all modes. Moreover, the LED light emission is polychromatic (typical spontaneous luminescence linewidth $\delta\lambda/\lambda\approx0.05$); even if the waveguide only supported one mode it would be extracted by the PhCs over some angular range. The design condition $k_{c,-1}=0$ should then be applied to a mid-order mode ($n_{effective}\approx2$), which results in $a'/\lambda=1/n_{effective}\approx0.5$ and a more directional light-extraction angle $\theta_e=24°$ (Figure 5b). Figure 5a–5c shows all the diffracted modes in the in-plane representation for $a'/\lambda=0.58$ and $a'/\lambda=0.5$, which illustrates the increase in directional light extraction achieved for $a'/\lambda=0.5$.

Off-axis modes propagating at an angle α can also be diffracted into the air cone (solid-red wave vectors in Figure 4c), with diffracted wave vector components along both the *a* and *c* directions, as well as polarization components E_a and E_c along both directions (Figure 4c). Along the next direction of symmetry, the *a* direction, the diffracted wave vectors $k_{a,-1}$ of off-axis modes (red dots in Figure 5a) have a sinusoidal dispersion relation $\lambda=a'n_{effective}\cos\alpha$ (see Supplementary Information).

The directional emission of $\vec{E}||\vec{a}$-polarized light along the *m*–*a* plane (observed in Figure 3c) is a result of the reduced excitation of the off-axis modes as α increases. The intensity of off-axis modes is proportional to their excitation by the P_x dipoles which decreases as $\cos^2\alpha$. The measured intensity of such modes after the polarization selection by the polarizer is also proportional to $\cos^2\alpha$, due to the angle α between the mode's polarization and polarizer aligned to the *a* direction. Finally, the intensity of light collected by the rotating optical fiber needs to be corrected by a term $\cos\theta$ that accounts for the change in solid angle with respect to θ (see Supplementary Information). This term also explains the angular response of the direct emission $I_{a,direct}(\theta)\propto\cos\theta$ observed from the sample without PhCs (Figure 3b). Combining all these terms with the direct polarized emission results in

$$I_{||a}(\theta) = I_{a,0}\cos^4\alpha\cos\theta + I_{a,direct}(\theta) \quad (3)$$

where α can also be expressed as a function of θ (see Supplementary Information).

From the same previous arguments, considering now a polarizer aligned to the *c* direction, the measured intensity of off-axis modes with $\vec{E}||\vec{c}$ polarization is $I_{||c}(\theta)=I_{c,0}\cos^2\alpha\sin^2\alpha\cos\theta+I_{c,direct}(\theta)$. This model is in good agreement with the experimental intensity of an extracted mode in the *m*–*a* plane for both *a* and *c* polarizations. Figure 6 shows the plot of the measured and calculated intensity versus angle using this model for both polarizations. The experimental intensity of a single mode ($n_{effective}=1.78$) with $\vec{E}||\vec{a}$ polarization was simply determined from the angle resolved measurement. For the $\vec{E}||\vec{c}$ polarization, the modes and their respective replicas are simultaneously present in the measurements (see Supplementary Figure S1b). The intensity of the $\vec{E}||\vec{c}$ polarization shown in Figure 6 therefore corresponds to intensities originating from several direct modes and their diffracted replicas. We compare the measurement with our model calculated for two different modes, with effective indexes of 1.1 and 2, which represent the range of extracted modes along the *m*–*a* plane with $\vec{E}||\vec{c}$ polarization.

The $\vec{E}||\vec{c}$ polarization, which is originally weak as it originates from the P_z dipole, benefits now from a component E_c from the strong dipole P_x that was propagating off-axis prior to diffraction by the PhCs. The contribution to the $\vec{E}||\vec{c}$ polarization from the P_z or P_x dipoles is distinguished by their wavelength, where longer wavelengths correspond to emission from P_x dipole and short wavelengths to P_z dipole[30] (see Supplementary Information).

The extraction of $\vec{E}||\vec{c}$ polarized light originated from the main P_x dipole does not deteriorate the polarization ratio of LEDs with 1D PhC

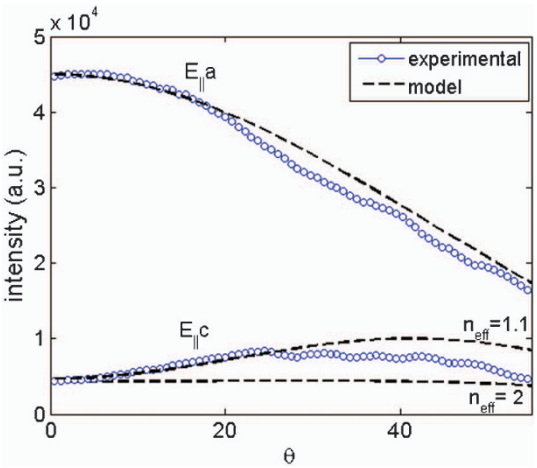

Figure 6 Intensity of extracted polarized modes. Measured intensity of an extracted mode in the *m*–*a* plane for both $\vec{E}||\vec{a}$ and $\vec{E}||\vec{c}$ polarizations along with the model of $I_{||a}(\theta)$ and $I_{||c}(\theta)$. For the $\vec{E}||\vec{a}$ polarization, an extra $\cos\theta$ term was included in equation (3) to account for the fact that the polarizer is aligned to the direction of rotation, therefore at $\theta=90°$, the polarizer is parallel to the *m* direction.

since it occurs mainly at large angles. However, if one were to use two-dimensional PhCs, the two-dimensional network of reciprocal points would result in more diffraction channels, increasing the projection of the strong polarization into the *c* direction. Moreover, the extraction of E_c would happen in smaller angles which would be more detrimental to the polarization ratio. A reduction in the period a' (or in the a'/λ ratio) of the 1D PhCs would not only increase the directional emission of polarized light but also diminish the extraction of $\vec{E}||\vec{c}$-polarized mode. A smaller a' (larger *G*) results in smaller in-plane angle α which reduces the intensity $I_{||c}$, even though in this case lower order modes are extracted in the *m*–*a* plane, which are generally better excited modes due to their larger overlap with the QWs.

CONCLUSIONS

We demonstrated in this paper a high-brightness polarized LED, achieved through the use of embedded PhCs. The air gap-embedded PhCs were introduced in *m*-plane GaN with a simple process, requiring only the patterning of the *m*-plane substrate prior to the LED growth by MOCVD. The resulting defect-free GaN layer coalesced over the embedded PhC is an important requirement for high-efficiency optoelectronic devices.

The polarization-preserving and directional light extraction properties from PhCs, along with the enhanced interaction of the embedded PhCs with the guided light, were combined to yield a directional polarized light emitting diode. We demonstrated that both direct and diffracted beams were highly polarized. A directional enhancement of the $\vec{E}||\vec{a}$-polarized emission, of up to 1.8-fold, was observed from the embedded PhCs with negligible changes in the $\vec{E}||\vec{c}$ polarization. A high degree of polarization of 88.7% at 465 nm was achieved.

Embedded PhCs offer a tool not only to increase polarized light emission in *m*-plane GaN LEDs, but to design their angular emission pattern. We discussed the important parameters to reduce even further the emission of $\vec{E}||\vec{c}$ polarization and to enhance the directional emission of the $\vec{E}||\vec{a}$ polarization, leading to polarized light emitters with higher brightness. This is not only desirable for LCD displays and polarized back-light sources in high efficiency TV displays and cell phones but also in general illumination, and could potentially lead the way to polarized white-light emitters.

ACKNOWLEDGMENTS

The experimental part of this work was performed at University of California, Santa Barbara. This study is based upon work partially supported as part of the 'Center for Energy Efficient Materials' at University of California, Santa Barbara, an Energy Frontier Research Center funded by the US Department of Energy, Office of Science, Office of Basic Energy Sciences under Award Number DE-SC0001009 and by the Solid State Lighting and Energy Center (SSLEC) at the University of California, Santa Barbara.

1 Pimputkar S, Speck JS, DenBaars SP, Nakamura S. Prospects for LED lighting. *Nat Photon* 2009; **3**: 180–182.
2 Clear R, Mistrick RG. Multilayer polarizers: a review of the claims. *J Illum Eng Soc* 1996; **25**: 70–88.
3 Japuntich DA. Polarized task lighting to reduce reflective glare in open-plan office cubicles. *Appl Ergon* 2001; **32**: 485–499.
4 Cornelissen HJ, Jagt HJ, Broer DJ, Bastiaansen CW. Efficient and cost-effective polarized-light backlights for LCDs. *Proc SPIE* 2008; **7058**: 70580X1.
5 Ecological Society of America. Polarized Light Leads Animals Astray: 'Ecological Traps' Cause Animal Behaviors That Can Lead To Death. ScienceDaily. Available at: http://www.sciencedaily.com/releases/2009/01/090107092714.htm (accessed 7 January 2009).
6 Chichibu S, Azuhata T, Sota T, Nakamura S. Spontaneous emission of localized excitons in InGaN single and multiquantum well structures. *Appl Phys Lett* 1996; **69**: 4188–4190.
7 Waltereit P, Brandt O, Trampert A, Grahn HT, Menniger J *et al*. Nitride semiconductors free of electrostatic fields for efficient white light-emitting diodes. *Nature* 2000; **406**: 865–868.
8 Chakraborty A, Haskell BA, Keller S, Speck JS, Denbaars SP *et al*. Demonstration of nonpolar *m*-plane InGaN/GaN light-emitting diodes on free-standing *m*-plane GaN substrates. *J Appl Phys* 2005; **44**: L173–L175.
9 Schmidt MC, Kim KC, Sato H, Fellows N, Masui H *et al*. High power and high external efficiency *m*-plane InGaN light emitting diodes. *J Appl Phys* 2007; **46**: L126–L128.
10 Gardner NF, Kim JC, Wierer JJ, Shen YC, Krames MR. Polarization anisotropy in the electroluminescence of *m*-plane InGaN–GaN multiple-quantum-well light-emitting diodes. *Appl Phys Lett* 2005; **86**: 111101.
11 Tsujimura H, Nakagawa S, Okamoto K, Ohta H. Characteristics of polarized electroluminescence from *m*-plane InGaN-based light emitting diodes. *J Appl Phys* 2007; **46**: L1010–L1012.
12 Kubota M, Okamoto K, Tanaka T, Ohta H. Temperature dependence of polarized photo-luminescence from nonpolar *m*-plane InGaN multiple quantum wells for blue laser diodes. *Appl Phys Lett* 2008; **92**: 011920.
13 Brinkley SE, Lin YD, Chakraborty A, Pfaff N, Cohen D *et al*. Polarized spontaneous emission from blue-green *m*-plane GaN-based light emitting diodes. *Appl Phys Lett* 2011; **98**: 011110.
14 Fujii T, Gao Y, Sharma R, Hu EL, DenBaars SP *et al*. Increase in the extraction efficiency of GaN-based light-emitting diodes via surface roughening. *Appl Phys Lett* 2004; **84**: 855–857.
15 Yamada M, Mitani T, Narukawa Y, Shioji S, Niki I *et al*. InGaN-based near-ultraviolet and blue light emitting diodes with high external quantum efficiency using a patterned sapphire substrate and a mesh electrode. *J Appl Phys* 2002; **41**: L1431–L1433.
16 Wierer JJ, David A, Megens MM. III-nitride photonic-crystal light-emitting diodes with high extraction efficiency. *Nat Photon* 2009; **3**: 163–169.
17 Matioli E, Rangel E, Iza M, Fleury B, Pfaff N *et al*. High extraction efficiency LED based on embedded air-gap photonic-crystals. *Appl Phys Lett* 2010; **96**: 031108.
18 DeMille NF, Denbaars SP, Nakamura S. Linearly polarized backlight source in conjunction with polarized phosphor emission screens for use in liquid crystal displays. US Patent 12/536,400, 5 August 2009.
19 Mulder CL, Reusswig PD, Beyler AP, Kim H, Rotschild C *et al*. Dye alignment in luminescent solar concentrators: II. Horizontal alignment for energy harvesting in linear polarizers. *Opt Express* 2010; **18**: A91.
20 Matioli E, Keller S, Wu F, Choi YS, Hu E *et al*. Growth of embedded photonic crystals for GaN-based optoelectronic devices. *J Appl Phys* 2009; **106**: 024309.
21 Getty A, Matioli E, Iza M, Weisbuch C, Speck J. Electroluminescent measurement of the internal quantum efficiency of light emitting diodes. *Appl Phys Lett* 2009; **94**: 181102.
22 Born M. *Atomic physics*. 8th ed. London: Blackie & Son Limited, 1969.
23 Ghosh S, Waltereit P, Brandt O, Grahn HT, Ploog KH. Electronic band structure of wurtzite GaN under biaxial strain in the *M* plane investigated with photoreflectance spectroscopy. *Phys. Rev B* 2002; **65**: 075202.
24 Sun YJ, Brandt O, Ramsteiner M, Grahn HT, Ploog KH. Polarization anisotropy of the photoluminescence of *m*-plane (In,Ga)N/GaN multiple quantum wells. *Appl Phys Lett* 2003; **82**: 22.
25 Matioli E, Fleury B, Rangel E, Melo T, Hu E *et al*. High extraction efficiency GaN-based photonic-crystal light-emitting diodes: comparison of extraction lengths between surface and embedded photonic-crystals. *Appl Phys Express* 2010; **3**: 032103.
26 Matioli E, Weisbuch C. Impact of photonic crystals on LED light extraction efficiency: approaches and limits to vertical structure designs. *J Phys D: Appl Phys* 2010; **43**: 354005.
27 David A, Benisty H, Weisbuch C. Optimization of light-diffracting photonic-crystals for high extraction efficiency LEDs. *J Display Technol* 2007; **3**: 133–148.
28 Lai CF, Chi JY, Yen HH, Kuo HC, Chao CH *et al*. Polarized light emission from photonic crystal light-emitting diodes. *Appl Phys Lett* 2008; **92**: 243118.
29 Jackson JD. *Classical electrodynamics*. New York: Wiley, 1998.
30 Matioli E, Brinkley S, Kelchner K, Nakamura S, DenBaars S *et al*. Polarized light extraction in m-plane GaN light-emitting diodes by embedded photonic crystals. *Appl Phys Lett* 2011; **98**: 251112.

Supplementary Information for this article can be found on *Light: Science & Applications*' website (http://www.nature.com/lsa/).